Numerical study of Yang-Mills classical solutions on the twisted torus

1993 J. Phys. A: Math. Gen. 26 2667

(http://iopscience.iop.org/0305-4470/26/11/015)

J. Phys. A: Math. Gen. 26 (1993) 2667–2678. Printed in the UK

Numerical study of Yang–Mills classical solutions on the twisted torus

M García Pérez and A González-Arroyo
Departmento Física Teórica C-XI, Universidad Autónoma de Madrid, Madrid 28049, Spain

Received 15 June 1992

Abstract. We use the lattice cooling method to investigate the structure of some gauge fixed SU(2) Yang–Mills classical solutions of the Euclidean equations of motion which are defined in the 3-torus with symmetric twisted boundary conditions.

1. Introduction

In this paper we will analyse an SU(2) Yang–Mills field configuration which is periodic in 3-space and tends to a pure gauge in both $t = \pm\infty$. This configuration is a solution of the classical Euclidean equations of motion and arises naturally when one studies gauge fields on the spatial torus with twisted boundary conditions (TBC) [1]. In particular, we fix the torus to have equal period in all three directions and a twist vector $\boldsymbol{m} = (1, 1, 1)$. The presence of the torus breaks the SO(3) rotational symmetry into the cubic group. If we fix, without loss of generality, the length of the spatial torus to $l = 1$, we may write the boundary conditions

$$\mathbf{A}_\mu(x + \hat{e}_i) = \sigma_i \mathbf{A}_\mu(x)\sigma_i \tag{1.1}$$

where σ_i are the Pauli matrices and $\hat{e}_i$ the unit vector in the ith direction. The choice of the Pauli matrices as the twist matrices can be regarded as a partial gauge fixing of the problem. The remaining group of gauge transformations must satisfy

$$\Omega(x + \hat{e}_i) = \sigma_i \Omega(x)\sigma_i . \tag{1.2}$$

This, however, is not the most general internal symmetry transformation of our problem. One can perform a transformation

$$\mathbf{A}_\mu(x) \to \mathbf{A}'_\mu(x) = \Omega^{(z)}(x)\mathbf{A}_\mu(x)\Omega^{(z)\dagger}(x) + \mathrm{i}\Omega^{(z)}(x)\partial_\mu\Omega^{(z)\dagger}(x) \tag{1.3}$$

with

$$\Omega^{(z)}(x + \hat{e}_i) = z_i\sigma_i\Omega^{(z)}(x)\sigma_i \tag{1.4}$$

and $z_i = \pm 1$. This transformation preserves the boundary condition (1.1) and leaves the Yang–Mills action invariant. Nevertheless, if $z_i \neq 1$ for some $i = 1, 2, 3$ the transformation is not, strictly speaking, a gauge transformation since it modifies the values of the Wilson loops associated with non-contractible loops (Polyakov loops):

$$W(\gamma) \to W'(\gamma) = z_i^{\omega_i(\gamma)} W(\gamma) \tag{1.5}$$

where $\omega_i(\gamma)$ is the winding number of the loop in the ith direction. We will call these transformations singular gauge transformations and the group of these transformations (modulo ordinary gauge transformations) is isomorphic to Z_2^3. As we will see later, these transformations act non-trivially on our gauge-field configuration.

The configuration with smallest action ($S = 0$) with our boundary conditions is of the pure gauge form

$$\mathbf{A}_\mu(x) = \mathrm{i}\Omega^{(z)}(x)\partial_\mu\Omega^{(z)\dagger}(x) \tag{1.6}$$

with $\Omega^{(z)}(x)$ satisfying equation (1.4). However, it turns out [2] that there are only two gauge non-equivalent configurations of this type, those with $z_i = 1$ for all i, and $z_i = -1$ for all i. In the $\mathbf{A}_0 = 0$ gauge these configurations are constant in time and equal to the minima of the potential energy $\sum_i \mathrm{Tr}\, B_i^2$. The problem becomes that of a Z_2 symmetric potential with two non-symmetric minima. The order parameter distinguishing these two is the Polyakov loop winding the torus once along each direction ($\omega_i = 1$). Just as in the case of the $\lambda\phi^4$ potential (and negative mass squared), we can investigate the solution which interpolates between the two minima as time goes from $-\infty$ to $+\infty$. This is an instanton solution and gives rise to the leading weak-coupling contribution to the energy splitting between the Z_2 symmetric and antisymmetric states.

These instanton configurations are precisely the solutions which we are after. They have half-integer topological charge and are precisely the minimum action configurations in a 4-torus with infinite length and with TBC both in time and space. The twist in time $n_{0i} = 1$ eliminates the constant minima solutions.

The existence of these configurations was proved by Sedlacek [3]. In a previous paper [4] we investigated the behaviour of these solutions by using the lattice approximation and the cooling method [5]. There it was shown that the total action and energy of the lattice minimum action configurations scale towards a continuum value. The value of the continuum action is very close to $4\pi^2$, the absolute minimum for a topological charge Q of $1/2$. Indeed, this minimum is only attained by a self-dual or anti-self-dual configuration, so our configurations must be very approximately, if not exactly, self-dual. If we perform a parity transformation to this self-dual instanton configuration we get an anti-self-dual anti-instanton configuration with $Q = -1/2$.

The purpose of this paper is to report a more extensive and accurate analysis of the lattice minimum configurations in order to answer some questions which were not settled by our previous paper. Apart from giving additional support to the question of scaling towards the continuum and self-duality, we have shown that there are indeed sixteen different gauge-inequivalent configurations (eight instantons and eight anti-instantons) which can be obtained by acting with the group of singular gauge transformations, parity and time reversal on one of them. All these configurations are non-Abelian and cubic-symmetric. We have obtained functional expressions for the various physical quantities, including the vector potentials and field strengths in a suitable gauge, which describe their qualitative features. Satisfactory quantitative description of the data has been obtained by using these functional expressions and the first few terms in a Fourier expansion of the functions involved. We also report the steps that we have taken in the direction of finding an analytic expression for the solution. Although our attempts in this respect have not achieved the ultimate goal, we have explored several paths involving some lenghthy and non-trivial manipulations, and our results can be of great help for future investigations.

Our solution, being non-Abelian, is very different to the Abelian solutions [6] which are known to exist for other twists, other values of the topological charge and additional periodicity in time. However, it is much more similar to the instanton solution on $S_3 \times \mathbb{R}$.

In a recent paper [7] this solution has been used to investigate the θ-dependence beyond the steepest descent. It is in this spirit that our solution is physically relevant. The reader is directed to [7] and the earlier [8] to see the role of our instanton solution for the Yang–Mills dynamics, in the weak-coupling limit. Its relevance beyond this limit is unknown.

2. Analysis of the data

Our strategy has been explained in [4]. We consider an $N_s^3 \times N_t$ lattice with TBCs. We use cooling to obtain configurations with smaller and smaller action. We stop once the value of the action has changed by less than 10^{-4} over the last 100 cooling sweeps. To perform the analysis reported here we have used the configurations which we employed in [4] together with new data which extend over larger lattices $(N_s, N_t) = (11, 29)$ and $(15, 29)$. We have little to add to the results of [4] concerning integrated quantities. The new data just give extra support to the conclusions presented there. The value of the action S is 39.234 and 39.347, for $(11, 29)$ and $(15, 29)$ in agreement with our extrapolation formula $S = 4\pi^2 - 29.7a^2$ (with $a = 1/N_s$). The degree of self-duality is now $X = 2|S_E - S_B|/S_E + S_B = 0.0045$ and 0.0033 for the same two lattices. We notice that the errors introduced by the lattice approximation are smaller than 1% for integral quantities. This can be explained by the fact that they are $\mathrm{O}(a^2)$. In the case of the vector potentials and the colour electric and magnetic fields at a given point $A_i^a(x)$, $E_i^a(x)$ and $B_i^a(x)$, we expect errors of order a: typically, then, 10% for our values of N_s. One can estimate more precisely the size of these errors by several methods. For example comparing E_i^a and B_i^a at the same point the difference is never greater than 0.14 (representing 3% of the magnitude at those points). On average a difference of order 0.04 makes the χ^2 per degree of freedom of the comparison of order 1. Other estimates of the errors can be deduced by comparing values for different N_s or by using different lattice approximants to the continuum value. The resulting errors depend on the quantity under consideration and on the value of t, but stay within a factor of two of 0.04 in all cases. We have chosen, thus, the value of 0.04 as a typical error which we will be using in all χ^2 fits of the data.

2.1. *Gauge-invariant quantities*

We start analysing the structure of our solution by looking at gauge-invariant quantities. Consider first the colour electric and magnetic fields E_i^a, B_i^a. They can be regarded as six vectors in the three-dimensional colour space. Gauge transformations amount to rotations in this space. Thus, the gauge-invariant quantities are the scalar products and moduli of these vectors $M_{ij} = \boldsymbol{E}_i \cdot \boldsymbol{E}_j$. Due to the approximate self-duality the colour magnetic fields give the same information within errors. Before stating the results of our analysis let us mention one technical point. Our interest is centred on the values of these quantities in the continuum limit. To extract these values one can use various lattice quantities all of which differ by an amount of order a. Nevertheless, in checking certain symmetries, it is essential to choose lattice observables which respect the lattice symmetry. For that reason we have extracted the colour field strength at each lattice point, $F_{\mu\nu}^b(na)$, by averaging the four plaquettes attached to that point in each $\mu\nu$ plane:

$$F_{\mu\nu}^b(na) = \frac{1}{4a^2}\,\mathrm{Tr}\{-\mathrm{i}\sigma_b[\mathbf{P}_{\mu\nu}(n) + \mathbf{P}_{\nu-\mu}(n) + \mathbf{P}_{-\nu\mu}(n) + \mathbf{P}_{-\mu-\nu}(n)]\} \quad (2.1)$$

where, for instance, $\mathbf{P}_{\nu-\mu}(n)$ stands for the following product of lattice links:

$$\mathbf{P}_{\nu-\mu}(n) = \mathbf{U}_\nu(n)\mathbf{U}_\mu^\dagger(n-\hat{\mu}+\hat{\nu})\mathbf{U}_\nu^\dagger(n-\hat{\mu})\mathbf{U}_\mu(n-\hat{\mu}).$$

The previous quantity transforms in the right way under gauge transformations and is symmetric under cubic transformations around the point na.

The main features of the solution are the following:

(i) At each time value there is a point of maximum energy density, which we will call the spatial centre of the instanton, whose coordinates are time-independent and we will choose them as $\boldsymbol{x} = \boldsymbol{0}$. Furthermore there is a time where the energy is maximal and we will choose it as the origin of time, $t = 0$. Our solution is cubic invariant with respect to the spatial centre and invariant under time reversal. The spatial centre is not one of the lattice points, but it can be located by interpolation. The same is true for the origin of time.

(ii) For all times and at the spatial centre of the instanton one has $M_{ij} \propto \delta_{ij}$. This orthogonality implies that the solution is not Abelian. Away from the centre the vectors E_i^a cease to be mutually orthogonal but they are never collinear.

(iii) We have fitted the moduli and scalar products at $t = 0$ to the first terms in a Fourier expansion. Our results are

$$\begin{aligned} M_{11} = \cos^2(\pi x)\{&15.00 + 20.02[\phi(y) + \phi(z)] - 3.12\cos^2(\pi y)\cos^2(\pi z) \\ &+ 0.128\sin^2(2\pi y)\sin^2(2\pi z) - 0.18[\cos^2(\pi y)\sin^2(2\pi z) \\ &+ \cos^2(\pi z)\sin^2(2\pi y)]\} + 32.74\phi(y)\phi(z) - \sin^2(2\pi x) \\ &\times \{0.232 + 2.25[\cos^2(\pi y) + \cos^2(\pi z)] + 0.80\cos^2(\pi y)\cos^2(\pi z)\} \end{aligned} \tag{2.2}$$

$$M_{12} = -1.608[1 - 0.433\cos(2\pi z)]\chi(x)\chi(y) \tag{2.3}$$

where

$$\phi(x) = \cos^2(\pi x) - 0.082\sin^2(2\pi x) \qquad \chi(x) = \sin(2\pi x) + 0.086\sin(4\pi x).$$

The quality of the fit is very good (see figure 1 for example). The remaining components are just obtained by the appropriate replacement of the indices and variables in the previous expression, in a way which is consistent with cubic invariance and parity invariance. Note that E_i^2 vanishes when $x_i = \pm 1/2$ and $x_j = \pm 1/2$. Note also that the solution seems perfectly smooth.

We turn now our attention to non-local gauge-invariant quantities: the Polyakov loops. Due to the boundary conditions these variables are defined as

$$\Omega_\mu(x) = T\exp\left\{\mathrm{i}\int_{\gamma_\mu(x,x')} \mathbf{A}_\nu\,\mathrm{d}x^\nu\right\}\Gamma_\mu(x')T\exp\left\{\mathrm{i}\int_{\gamma_\mu(x',x)} \mathbf{A}_\nu\,\mathrm{d}x^\nu\right\} \tag{2.4}$$

where $\gamma_\mu(a, b)$ is a straight line in the positive μ direction starting at a and ending at b, x' is the border of the torus patch, $T\exp$ is the ordered exponential and $\Gamma_\mu(x)$ the twist matrices. On the lattice these quantities are simply given by the ordered product of the μ-links corresponding to the path $\gamma_\mu(x)$. These quantities transform like $\mathbf{E}_i$ under gauge transformations and therefore the gauge-invariant quantities are just the scalar products in colour space $\frac{1}{2}\operatorname{Tr}(\Omega_\mu(x)\Omega_\nu(x)) = X_{\mu\nu}(x)$ and the traces themselves $\frac{1}{2}\operatorname{Tr}(\Omega_\mu(x)) = X_\mu(x)$.

Since our instanton evolves in time from one pure gauge (1.6) ($z_i = 1$) to another gauge-inequivalent one ($z_i = -1$), and a representative of each class is given by $\Omega_i(x) = \pm\mathrm{i}\sigma_i (i = 1, 2, 3)$, we expect $X_{ij} = -\delta_{ij}$, $X_i = 0$ for large $|t|$. Indeed our results agree with this situation. As a matter of fact X_μ can be fitted with a $\chi^2 = 0.005$ per degree of freedom (with an absolute error of 0.04) to the formula

$$X_\mu = \prod_{\nu \neq \mu} m_\nu \tag{2.5}$$

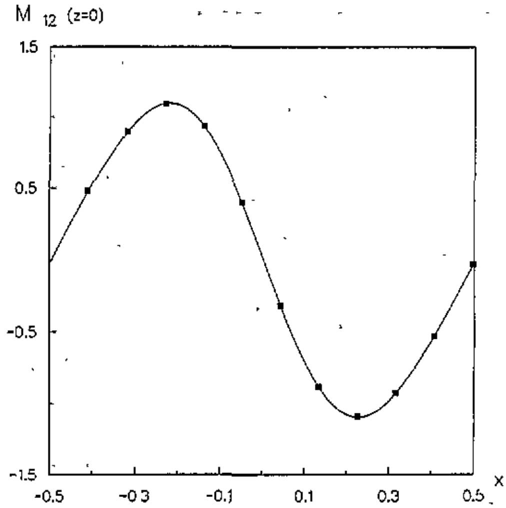

Figure 1. The scalar product $M_{12} = E_1 \cdot E_2$ plotted as a function of x for $y = 0.209$ and $z = 0$. The squares correspond to the lattice values for $N_s = 11$, $N_t = 21$. They are compared with the prediction of equation (2.3).

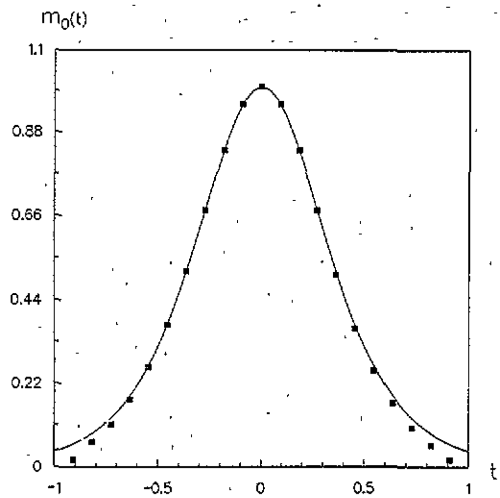

Figure 2. $m_0(t)$ appearing in equation (2.5) is plotted as a function of time for $N_s = 11$, $N_t = 21$. The full curve represents the function $\cos(\frac{1}{2}\pi \tanh(0.69\pi t))$.

where $m_i = m(x_i)$ for $i = 1, 2, 3$ and $m_0 = m_0(t)$. This is a very remarkable factorization property. The function m is parametrized as

$$m(x) = \cos(\pi x)(1 + C \sin^2(\pi x)) \tag{2.6}$$

where $C = -0.196$ and $m_0(t)$ is given in figure 2. Note as well that the m functions are antiperiodic. Thus, by translating our solution by one period in any direction we get a new solution. In this fashion one generates four solutions out of one. Thus, we are not dealing with a unique instanton solution but rather with a family of solutions related by singular gauge transformations.

2.2. *Gauge-dependent quantities*

In order to extract all the information from our numerical results we also have to obtain gauge-dependent information. In particular, one would like to extract the gauge potentials themselves in a suitable gauge. This turns out to be feasible and our results are presented in what follows.

First of all one must introduce a simple gauge fixing, which respects most of the symmetry of the problem. It is natural to select $\mathbf{A}_0 = 0$, a condition which preserves all spatial symmetries. To completely specify the gauge one has to fix the remaining time-independent gauge transformations. This can be done by fixing $A(x, t = -\infty) = \boldsymbol{0}$ or equivalently $\boldsymbol{\Omega}_i(x, t = -\infty) = \mathrm{i}\sigma_i$. This fixes the gauge completely including global gauge rotations. At $t = +\infty$ the gauge fields must coincide with a pure gauge (1.6) and in the $\mathbf{A}_0 = 0$ gauge this gauge transformation is indeed given by the temporal Polyakov loop $\boldsymbol{\Omega}_0(x, t = -\infty)$. Notice that $\boldsymbol{\Omega}_0$ transforms precisely like equation (1.4) for $z_i = -1$. The exact form of $\boldsymbol{\Omega}_0(x, t = -\infty)$ can be obtained in terms of the gauge-invariant quantities $\frac{1}{2}\mathrm{Tr}(\boldsymbol{\Omega}_0(x, t = -\infty))$ and $\frac{1}{2}\mathrm{Tr}(\boldsymbol{\Omega}_0(x, t = -\infty) \cdot \boldsymbol{\Omega}_i(x, t = -\infty))$. These have been obtained from our data and the result can be summarized by giving a functional form which describes these data with a $\chi^2 = 0.01$ per degree of freedom

$$\Omega_0(x, t = -\infty) = m(x)m(y)m(z)I + \mathrm{i}\sqrt{1 - \prod_i m_i^2}\,\frac{f \cdot \sigma}{|f|} \tag{2.7}$$

where $f_i = f(x_i)$ and $f(x) = \sin(\pi x)(1 + B\cos^2(\pi x))$, with $B = -0.172$. Notice that $f(x)$ is very similar to $m(x + 1/2)$. Changing the value of B to C does not significantly change the quality of the fit.

Now we turn our interest towards computing $\mathbf{A}_i(x, t)$ in the previously mentioned gauge. To extract these quantities from our lattice results implies some lengthy procedure. Apart from the typical order a errors we have to deal with some other sources of errors. Some errors arise through the gauge-fixing procedure due to the finite value of N_t/N_s. In this case $\mathbf{A}_i$ is never a pure gauge and cannot be set to zero. Nevertheless these errors are, for most purposes, quite small and can be monitored by varying N_t/N_s. Our procedure to evaluate the gauge fixing on the lattice configuration is as follows. To evaluate the gauge-fixed value of a lattice link $\mathbf{U}_\mu(n)$, we choose a lattice path going through this link and starting and ending at some point P. This point is situated on the surface of minimum energy (smallest time $n_t = -(N_t - 1)/2$) and the path is made of three parts γ_1, γ_2 and γ_3. The first and last paths are situated on the surface of time coordinate $-(N_t - 1)/2$. γ_1 joins P with $P' = (-(N_t - 1)/2, \boldsymbol{n})$, the point with equal spatial coordinates as the origin of the link $\mathbf{U}_\mu(n)$. γ_3 joins $P'' = (-\frac{1}{2}(N_t - 1), \boldsymbol{n} + \hat{\mu})$ with P. γ_2 moves from P' along the positive time direction, then goes through the link in question, and then back to P'' along the negative time direction. We complete our gauge fixing by performing a global gauge transformation $\Omega(P)$ which rotates the spatial Polyakov loops Ω_i starting at point P to the values $i\sigma_i$. Summarizing these transformations we write down the expressions for the gauge transformed link $\mathbf{U}'_\mu(n)$:

$$\mathbf{U}'_\mu(n) = \Omega(P)\mathbf{U}_{\gamma_1}\mathbf{U}_{\gamma_2}\mathbf{U}_{\gamma_3}\Omega^\dagger(P). \tag{2.8}$$

Indeed, if the spatial links at the smallest time are a pure gauge configuration, $\mathbf{U}_{\gamma_1}$ and $\mathbf{U}_{\gamma_3}$ can be gauged to I. Since in the temporal gauge $\mathbf{U}_{\gamma_2} = \mathbf{U}_\mu(n)$, we see that $\mathbf{U}'_\mu(n)$ is really our gauge fixed link.

In addition, the position of P and the choice of γ_1 and γ_3 are irrelevant. However, as mentioned previously, we do not exactly have a pure spatial gauge for $-(N_t - 1)/2$ and the actual choice of γ_1 and γ_3 is relevant. To preserve the fact that $\mathbf{U}'_\mu(n)$ (Eq.(2.8)) is a gauge transform of $\mathbf{U}_\mu(n)$, one must choose P, γ_1 and γ_3 in a predetermined way for all lattice links. Our choice is as follows. The path γ_1 is obtained by running first in the 1 direction, next in the 2 direction and finally in the 3 direction. We finally obtain

$$\mathbf{U}'_\mu(n) = \Omega(P)\mathbf{L}(n)\mathbf{U}_\mu(n)\mathbf{L}^\dagger(n + \hat{\mu})\Omega^\dagger(P) \tag{2.9}$$

with

$$\begin{aligned}\mathbf{L}(n) = {} & \prod_{q_1=0}^{n'_1-1}\mathbf{U}_1(P + q_1\hat{e}_1)\prod_{q_2=0}^{n'_2-1}\mathbf{U}_2(P + n'_1\hat{e}_1 + q_2\hat{e}_2)\prod_{q_3=0}^{n'_3-1}\mathbf{U}_3(P + n'_1\hat{e}_1 + n'_2\hat{e}_2 + q_3\hat{e}_3) \\ & \times\prod_{q_0=0}^{n'_0-1}\mathbf{U}_0(P + n'_1\hat{e}_1 + n'_2\hat{e}_2 + n'_3\hat{e}_3 + q_0\hat{e}_0)\end{aligned} \tag{2.10}$$

where $n'_\mu = n_\mu - P_\mu$ and P_μ are the coordinates of point P.

Once the data are gauge fixed we can extract the lattice approximants to the continuum fields. The potentials A_i^a are taken to lie on the mid-point of the corresponding links. The magnetic fields B_i^a, are computed by the plaquette averages mentioned before. Our results show the same qualitative features for both vector potentials and magnetic fields. These features are described by the following functional form which fits the data:

$$O_1^1 = q_1(t)\cos(\pi y)\cos(\pi z)(1+q_2(t)\cos(2\pi x))(1+q_3(t)\cos(2\pi y))(1+q_3(t)\cos(2\pi z))$$

$$O_1^2 = (1+a_1(t)\cos(2\pi x))(1+a_2(t)\cos(2\pi z))[a_3(t)\sin(\pi z)\cos(\pi x)(1+a_4(t)\cos(2\pi y)) + a_5(t)\cos(\pi z)\sin(\pi x)\sin(2\pi y)] \tag{2.11}$$

$$O_1^3 = (1+a_1(t)\cos(2\pi x))\,(1+a_2(t)\cos(2\pi y))[-a_3(t)\sin(\pi y)\cos(\pi x)(1+a_4(t)\cos(2\pi z)) + a_5(t)\cos(\pi y)\sin(\pi x)\sin(2\pi z)]$$

where O_i^a stands for either B_i^a, E_i^a or A_i^a, but with different values of the parameters q_i and a_i. The remaining components of O_i^a can be obtained by cyclic permutations of the indices $1, 2, 3$ in equation (2.11). The values of the parameters appearing in the expression are given in tables 1 to 4.

Table 1. The value of the parameters obtained when fitting the functional form (2.11) and (3.2) to the $N_s = 11$, $N_t = 29$ data for A_1^1. $n_t = 15$ corresponds to the time of maximum energy. Errors are indicated by giving, within parentheses, the magnitude which affects the last quoted digit.

nt	q_1	q_2	q_3	q_4
5	0.094(8)	0.04(6)	0.02(6)	0.00(1)
6	0.140(8)	0.05(2)	0.02(2)	0.00(1)
7	0.208(8)	0.06(3)	0.02(3)	0.00(1)
8	0.302(8)	0.07(2)	0.02(2)	0.00(1)
9	0.438(8)	0.09(1)	0.03(2)	0.00(1)
10	0.624(8)	0.103(9)	0.043(9)	0.00(1)
11	0.870(8)	0.120(6)	0.058(7)	0.01(1)
12	1.182(6)	0.138(4)	0.078(5)	0.02(1)
13	1.550(6)	0.154(3)	0.102(4)	0.02(1)
14	1.954(6)	0.167(3)	0.129(3)	0.03(1)
15	2.356(6)	0.177(1)	0.156(2)	0.05(1)
16	2.716(6)	0.182(2)	0.182(2)	0.07(1)
17	3.010(6)	0.184(1)	0.205(2)	0.09(1)
18	3.234(6)	0.183(1)	0.224(2)	0.11(1)
19	3.392(6)	0.181(1)	0.240(2)	0.12(1)
20	3.498(6)	0.179(1)	0.252(2)	0.13(1)
21	3.566(6)	0.178(1)	0.261(2)	0.14(1)
22	3.610(6)	0.176(1)	0.267(2)	0.14(1)
23	3.638(6)	0.175(1)	0.272(2)	0.14(1)
24	3.654(6)	0.174(1)	0.276(2)	0.14(1)
25	3.664(6)	0.174(1)	0.278(2)	0.14(1)
26	3.672(6)	0.173(1)	0.280(2)	0.14(1)
27	3.674(6)	0.173(1)	0.282(2)	0.14(1)
29	3.674(6)	0.172(1)	0.284(2)	0.14(1)

Table 2. The same as table 1 but for the parameters entering in A_1^2, A_1^3.

nt	a_1	a_2	a_3	a_4	a_5
6	0.00(6)	−0.02(6)	−0.122(6)	0.07(4)	−0.002(6)
7	0.01(5)	−0.03(4)	−0.172(6)	0.09(3)	0.008(6)
8	0.01(3)	0.01(3)	−0.244(6)	0.11(2)	0.018(6)
9	0.01(2)	0.03(2)	−0.348(6)	0.14(2)	0.034(6)
10	0.02(1)	0.04(1)	−0.496(6)	0.15(1)	0.062(6)
11	0.02(8)	0.07(1)	−0.704(6)	0.19(8)	0.109(6)
12	0.033(6)	0.092(5)	−0.984(6)	0.225(6)	0.174(6)
13	0.042(5)	0.118(5)	−1.344(6)	0.253(4)	0.272(6)
14	0.052(4)	0.145(4)	−1.776(6)	0.278(3)	0.402(6)
15	0.060(3)	0.169(3)	−2.258(6)	0.298(3)	0.558(6)
16	0.065(3)	0.189(2)	−2.746(6)	0.311(2)	0.730(6)
17	0.068(2)	0.204(2)	−3.200(6)	0.314(2)	0.902(6)
18	0.069(2)	0.215(2)	−3.590(6)	0.324(2)	1.056(6)
19	0.069(2)	0.221(2)	−3.902(6)	0.325(2)	1.186(6)
20	0.067(2)	0.225(1)	−4.138(6)	0.325(1)	1.290(6)
21	0.065(2)	0.227(2)	−4.312(6)	0.324(1)	1.368(6)
22	0.064(2)	0.229(1)	−4.434(6)	0.323(1)	1.424(6)
23	0.063(2)	0.230(1)	−4.520(6)	0.322(1)	1.436(6)
24	0.062(2)	0.230(1)	−4.580(6)	0.321(1)	1.494(6)
25	0.061(2)	0.231(1)	−4.620(6)	0.320(1)	1.514(6)
26	0.061(2)	0.231(1)	−4.648(6)	0.320(1)	1.530(6)
27	0.061(2)	0.231(1)	−4.666(6)	0.320(1)	1.540(6)
29	0.061(2)	0.232(1)	−4.686(6)	0.320(1)	1.554(6)

Table 3. The same as table 1 but for the data of B_1^1.

nt	q_1	q_2	q_3	q_4
3	0.216(8)	0.04(3)	0.00(3)	0.00(1)
5	0.424(8)	0.06(1)	0.01(2)	0.00(1)
6	0.610(8)	0.07(8)	0.02(1)	0.00(1)
7	0.876(8)	0.090(5)	0.026(8)	0.00(1)
8	1.246(8)	0.109(4)	0.038(6)	0.01(1)
9	1.736(8)	0.130(3)	0.054(4)	0.01(1)
10	2.352(8)	0.152(2)	0.077(3)	0.03(1)
11	3.058(8)	0.175(2)	0.107(2)	0.05(1)
12	3.760(8)	0.196(1)	0.144(2)	0.08(1)
13	4.300(8)	0.213(1)	0.191(2)	0.12(1)
14	4.504(8)	0.223(1)	0.244(2)	0.17(1)
15	4.278(6)	0.224(1)	0.301(2)	0.21(1)
16	3.682(8)	0.216(1)	0.361(2)	0.23(1)
17	2.900(8)	0.200(2)	0.421(2)	0.21(1)
18	2.124(8)	0.181(2)	0.482(3)	0.17(1)
19	1.474(6)	0.160(3)	0.542(5)	0.12(1)
20	0.986(6)	0.141(4)	0.603(7)	0.08(1)
21	0.644(6)	0.124(6)	0.663(1)	0.04(1)
22	0.412(6)	0.108(8)	0.73(1)	0.03(1)
23	0.264(6)	0.09(1)	0.79(3)	0.01(1)
24	0.166(6)	0.08(2)	0.87(4)	0.00(1)
26	0.062(6)	0.03(4)	1.1(1)	0.00(1)

The previous functional form satisfactorily describes the data with a maximum χ^2 per degree of freedom equal to 4 for A_l^a and 6 for B_l^a. It can be used to study the main features

Table 4. The same as table 2 but for the data of B_1^2, B_1^3.

nt	a_1	a_2	a_3	a_4	a_5
3	0.00(6)	0.00(6)	−0.120(6)	0.07(4)	0.006(6)
5	0.01(2)	0.02(3)	−0.292(6)	0.10(2)	0.022(6)
6	0.01(2)	0.02(2)	−0.438(6)	0.12(1)	0.042(6)
7	0.02(1)	0.04(1)	−0.644(4)	0.147(8)	0.074(6)
8	0.019(2)	0.050(8)	−0.940(6)	0.177(6)	0.132(6)
9	0.027(5)	0.069(5)	−1.354(6)	0.210(4)	0.224(6)
10	0.037(4)	0.095(4)	−1.912(3)	0.245(3)	0.370(6)
11	0.050(3)	0.126(3)	−2.626(6)	0.280(2)	0.584(6)
12	0.064(2)	0.161(2)	−3.464(6)	0.313(2)	0.872(6)
13	0.079(2)	0.198(1)	−4.322(6)	0.341(1)	1.212(6)
14	0.092(2)	0.233(1)	−5.018(6)	0.361(1)	1.550(6)
15	0.100(2)	0.262(1)	−5.354(6)	0.372(1)	1.796(6)
16	0.100(2)	0.282(1)	−5.214(6)	0.372(1)	1.880(6)
17	0.093(2)	0.293(1)	−4.754(6)	0.364(1)	1.786(6)
18	0.080(2)	0.297(2)	−3.950(6)	0.349(2)	1.556(6)
19	0.064(3)	0.294(2)	−2.998(6)	0.331(2)	1.264(6)
20	0.047(4)	0.289(3)	−2.232(6)	0.312(3)	0.974(6)
21	0.031(5)	0.282(4)	−1.608(6)	0.293(4)	0.724(6)
22	0.017(7)	0.276(6)	−1.132(6)	0.277(3)	0.522(6)
23	0.00(1)	0.271(8)	−0.784(6)	0.264(8)	0.370(6)
24	0.00(1)	0.27(1)	−0.536(3)	0.26(1)	0.230(6)
25	0.00(2)	0.28(1)	−0.364(6)	0.26(2)	0.180(6)
26	0.00(3)	0.30(2)	−0.244(6)	0.27(3)	0.130(6)
29	0.00(3)	0.30(2)	−0.244(6)	0.27(3)	0.130(6)

of the solution. Another interesting aspect of the formula is that it can serve as a guide to the construction of an ansatz which could lead to an analytic expression of the solution. In the following section we will describe the steps that we have taken in this direction.

3. Ansatz

In equation (2.11) we have given an analytic expression which describes our numerical results within errors. It is clear that the solution is not as simple as that expression, but we want to explore the consequence of the fact that it shares with it the same behaviour under the symmetry operations of the system. Thus, we will assume the following general form for the solution (for all t):

$$A_i^a = \delta_i^a Q^{(1)}(t, x_i, x_j, x_k) + (\epsilon^{iab})^2 Q^{(2)}(t, x_i, x_a, x_b) + \epsilon^{iab} Q^{(3)}(t, x_i, x_a, x_b) \tag{3.1}$$

where $Q^{(1)}(t, x, y, z) = Q^{(1+)}(t, x, y, z)$ is symmetric under the exchange of y and z, even in all the three variables, antiperiodic in y and z, periodic in x. $Q^{(2)}(t, x, y, z)$ is odd in x,y, even in z, antiperiodic in x,z and periodic in y. $Q^{(3)}(t, x, y, z)$ is odd in the third variable and even in the other two, antiperiodic in x,z and periodic in y. The previous expression implies that the solution is cubic symmetric with $A_i^a(x)$ and $B_i^a(x)$ transforming in the $T_1 \otimes T_1$ representation of this group (T_1 is just the spin-1 representation of rotations). In addition, the behaviour under translations by one period is just what is required by the TBC. The previous properties are more restrictive than what can be deduced by these symmetry properties alone. More precisely $Q^{(1)}(t, x, y, z)$ could contain an additional term $Q^{(1-)}(t, x, y, z)$ which is odd in all three variables, antiperiodic and antisymmetric in the two last variables y,z. To test the presence or absence of this term we have added to A_1^1 in the parametrization equation (2.11) a term

$$q_4 \sin(2\pi x)\sin(\pi y)\sin(\pi z)(\cos(2\pi y) - \cos(2\pi z)) \tag{3.2}$$

and refitted our data for **A** and **B**. The presence of a such a term improves the value of the χ^2 by a factor 2/5, but the size of q_4 and thus its contribution is of the order of the estimated size of the O(a) errors. Thus, we will keep an open attitude and explore both possibilities.

Other additional information which might be crucial for finding the analytic expression is the behaviour under $P \cdot T$. Both parity and time reversal map instantons into anti-instantons, but one could ask whether the product of these two leaves our solution invariant or not. The implications of this invariance are complicated by the future–past asymmetry of our gauge choice. Invariance under $P \cdot T$ implies

$$-\mathbf{A}_i(-x, -t) = \Omega_0^\dagger \mathbf{A}_i(x, t)\Omega_0 + \mathrm{i}\Omega_0^\dagger \partial_i \Omega_0 \tag{3.3}$$

where Ω_0 is the gauge matrix which describes the pure gauge at $t = \infty$. The matrix Ω_0 was parametrized by equation (2.7) and indeed the form of the axis of rotation $f/|f|$ is precisely consistent with the restricted form where $Q^{(1)} = Q^{(1+)}$ even in all three variables. The necessary and sufficient condition for the gauge field at ∞ to be of the restricted form $Q^{(1-)} = 0$ is that f_i is a function of x_i alone.

Expression (3.3) conflicts nevertheless with the requirement $Q^{(1-)} = 0$ since, in principle, a rotation by Ω_0 does not preserve this constraint. If we impose the condition that a general rotation around $f/|f|$ should preserve $Q^{(1-)} = 0$ we must have

$$Q^{(2)}(t, x, y, z) = f(y)\hat{Q}^{(2)}(t, x, y, z) \tag{3.4}$$

$$Q^{(3)}(t, x, y, z) = f(z)\hat{Q}^{(3)}(t, x, y, z) \tag{3.5}$$

where $\hat{Q}^{(2)}(t, x, y, z)$ and $\hat{Q}^{(3)}(t, x, y, z)$ are symmetric functions of the last two arguments y,z. We have verified that these additional constraints are reasonably well satisfied by our data. Thus, we arrive at a restricted parametrization consistent with our data:

$$A_i^a(x, t) = \rho_1^i \frac{f_i f_a}{|f|} + \rho_2^i |f| \left(\delta_i^a - \frac{f_i f_a}{|f|^2}\right) + \rho_3^i \epsilon_{abi} f_b \tag{3.6}$$

where ρ_1^i, ρ_2^i and ρ_3^i must be even functions of the three variables x, y, z. ρ_1^i and ρ_2^i are periodic in x_i and antiperiodic in $x_j \neq x_i$, and ρ_3^i is antiperiodic in x_i and periodic in $x_j \neq x_i$.

The fact that this form is not a mere consequence of the symmetry properties implies that, when requiring self-duality of such a solution, new equations will arise which guarantee the form to be preserved.

To start with, let us perform a time-independent gauge transformation and write

$$\mathbf{A}_i'(x, t) = \Omega_0^{-1/2}\mathbf{A}_i(x, t)\Omega_0^{1/2} + \mathrm{i}\Omega_0^{-1/2}\partial_i \Omega_0^{1/2}. \tag{3.7}$$

This new vector potential also complies to the form (3.6) with respect to the behaviour of the ρ' functions under parity. In addition it must satisfy $-\mathbf{A}_i'(-x, -t) = \mathbf{A}_i'(x, t)$. This implies that $\rho_1'^i$ and $\rho_2'^i$ are odd in t and $\rho_3'^i$ is even in t. We have explicitly checked these properties in our numerical data and found agreement within errors. In fact, given self-duality it is enough that $\rho_1^{\prime i} = \rho_2^{\prime i} = 0$ at $t = 0$ to guarantee the appropiate behaviour for $t \neq 0$. At $t = 0$ we have been able to fit both $\mathbf{A}_i$ and $\mathbf{B}_i$ with $\rho_3^{\prime i}$ alone.

Now imposing self-duality we obtain six equations rather than three. The first set of equations follows from the requirement that the ρ_a^i should have the required behaviour under parity. The equations are

$$\epsilon^{ijk}(\nabla_j \hat{\rho}_a^k + T^{abc} \hat{\rho}_b^j \hat{\rho}_c^k) = 0 \tag{3.8}$$

where $\nabla_j = (1/f_j)\partial_j$, $\hat{\rho}_a^i = \rho_a^i + \delta_{a3}\partial_i(f(x_i))/(2|f|^2)$ and T^{abc} is a completely antisymmetric tensor with $-T^{123} = T^{231} = T^{312} = 1$.

The solution to this equation is as follows

$$\hat{\rho}_a^i = R^{a\rho\sigma} q_\rho \nabla_i q_\sigma \tag{3.9}$$

where q_ρ satisfy $q_1^2 + q_2^2 - q_3^2 - q_4^2 = 1$ and $R^{a\rho\sigma}$ is a tensor, antisymmetric in the last two indices, with $R^{121} = R^{134} = R^{213} = R^{242} = R^{314} = R^{323} = 1$. The functions q_μ then establish a mapping from $S_1^3 \times \mathbb{R}$ onto that hyperboloid.

If we now plug the solution for $\hat{\rho}$ (equation (3.9)) into the self-duality equation, and after considerable massaging, we arrive at

$$\partial_0 s^a = \epsilon^{abc} s_b s_c' \tag{3.10}$$

$$\nabla_i s_a' = \nabla_j \nabla_k s_a \qquad \forall i \neq j \neq k \tag{3.11}$$

$$s^a s_a = |f|^2 \tag{3.12}$$

where indices are raised and lowered with the metric $g_{ab} = \mathrm{diag}(1, -1, -1)$ and $s_1 = |f|(q_1^2 + q_2^2 + q_3^2 + q_4^2)$, $s_2 = 2|f|(q_2q_3 - q_1q_4)$ and $s_3 = 2|f|(q_1q_3 + q_2q_4)$. The dynamics (3.10) is consistent with the constraint (3.12). The most important restriction follows from the integrability condition of (3.11), which together with (3.12) serves to restrict the possible value of $f(x)$. If we introduce the function $z_i \equiv z(x_i)$ by the condition $\mathrm{d}z(x)/\mathrm{d}x = f(x)$, equation (3.11) forces s_a to be a sum of single variable functions of the variables $a_1z_1 + a_2z_2 + a_3z_3$ with $a_i = +1, -1$ or 0 and $\sum a_i = 1 (\mathrm{mod}\ 2)$. On the other hand, $|f|^2$ is a sum $F(z_1) + F(z_2) + F(z_3)$. One class of solutions is given by functions $s_a(z_1+z_2+z_3)$. In this case (3.12) forces $f(x) = Ax$ and then the whole problem possesses spherical symmetry $z_1 + z_2 + z_3 \propto |x|^2$. We are then in the situation discussed in [9] and our equations recover all the axially symmetric solutions including the BPST [10] one. It is not easy to find other solutions to equations (3.11) and (3.12). Indeed, if we impose these conditions on the coefficients of the Taylor expansion of the functions $s_a(z)$, the number of conditions grows faster than the number of parameters. This suggests trying polynomials for the functions s_a. In this way we have discovered other solutions, most remarkably one which is defined on the torus with $z = A\cos(Bx + C)$ and where s_1 and s_3 are polynomials of second degree in z_i and s_2 of first degree. The solution goes to a pure gauge in $t \to \pm\infty$ but is singular at $t = 0$ and the total action is divergent (in the unit cell). We have been unable to find any solution which is satisfactory and coincides with our numerical data.

If our solution does not follow from equations (3.10)–(3.12), one has to drop some of the assumptions leading to those equations. Most probably it is equation (3.6) with the assumed properties for ρ_a^i which is wrong, since its validity is simply based on the ability to describe the data. Unfortunately, if we go back to the form (3.1) with $Q^{(1)} = Q^{(1+)} + Q^{(1-)}$ we have no additional equations which could allow an analytic development analogous to that leading to equations (3.10)–(3.12). One can simply rewrite the self-duality equations for the Q functions, but we do not know how to select solutions going to a pure gauge in $t = \pm\infty$.

4. Summary and conclusions

In this paper, we have studied the instanton-like solution which occurs in a 3-torus with symmetric twist. It is remarkable that the cooling method provides a very accurate description of this solution which allows a systematic analysis of its properties. Our results imply that, with our boundary condition $\mathbf{A}_i = 0$ at $t = -\infty$, there are indeed four instanton and four anti-instanton solutions, all of which are (within errors) cubic symmetric and $P \cdot T$ invariant (another set of eight solutions satisfying $\mathbf{A}_i = 0$ at $t = +\infty$ are obtained by time reversal). The solution is also smooth, although singularities in sufficiently high derivatives are not excluded. We have given functional forms which incorporate the previously mentioned properties, plus additional restrictions consistent with the data. Nonetheless, the more restrictive form, which allows the reduction of the problem to motion on a hyperboloid and recovers many multi-instanton solutions on S_4 does not seem to contain the solution of our problem.

Acknowledgment

This work has been partially financed by CICYT.

References

[1] 't Hooft G 1979 *Nucl. Phys.* **153** 141; 1980 *Acta Phys. Austriaca Suppl.* **22** 531
[2] González-Arroyo A and Korthals Altes C P 1988/89 *Nuc. Phys.* B **311** 433
[3] Sedlacek S 1982 *Commun. Math. Phys.* **86** 515
[4] Garc'ia Pérez M, González-Arroyo A and Söderberg B 1990 *Phys. Lett.* **235B** 117
[5] Berg B 1981 *Phys. Lett.* **104B** 61
Teper M 1985 *Phys. Lett.* **162B** 357
[6] 't Hooft G 1981 *Commun. Math. Phys.* **81** 267
van Baal P 1984 Twisted boundary conditions: a non perturbative probe for pure non-Abelian gauge theories *Ph D Thesis* Utrecht
[7] van Baal P and Hari Dass N D 1992 *Nucl. Phys.* B **385** 185
[8] Hansson T, van Baal P and Zahed I 1987 *Nucl. Phys.* B **289** 682
Daniel D, González-Arroyo A, Korthals Altes C P and Söderberg B 1989 *Phys. Lett.* **221B** 136
[9] Witten E 1977 *Phys. Rev. Lett.* **38** 121
[10] Belavin A, Polyakov A M, Schwartz A S and Tyupkin Yu S 1975 *Phys. Lett.* **59B** 85